Acta of Bioengineering and Biomechanics
Vol. 27, No. 4, 2025

Original paper
DOI: 10.37190/abb/217504

Mechanical evaluation of additively manufactured polymer rings for circular external fixators

BARTOSZ MARTYNIUK[1]*, DOMINIKA REJNIAK[2],
PIOTR MORASIEWICZ[3], JAROSŁAW FILIPIAK[1]

[1] Department of Mechanics, Materials and Biomedical Engineering,
Wrocław University of Science and Technology, Wrocław, Poland.
[2] Wrocław University of Science and Technology, Wrocław, Poland.
[3] Department of Orthopaedic and Trauma Surgery, Institute of Medical Sciences,
University of Opole, Opole, Poland.

Purpose: The aim of this study was to assess the feasibility of using additively manufactured polymer rings as structural components of circular external fixators for limb lengthening in pediatric patients. The analysis focused on whether such rings can provide sufficient mechanical performance while simultaneously reducing device mass and improving radiographic transparency compared with conventional metallic solutions. *Methods*: Two design variants of circular rings with different cross-sectional geometries were developed and manufactured using fused filament fabrication from a thermoplastic polymer. Their mechanical behavior was assessed through numerical finite element simulations and experimental testing. Radial and axial loading conditions corresponding to clinical use were analyzed at the ring level. Subsequently, complete external fixator assemblies incorporating the printed rings were constructed and subjected to quasi static axial compression tests. Comparative radiographic imaging was also conducted to evaluate the influence of polymer-based rings on image quality relative to conventional aluminum rings. *Results*: The polymer rings exhibited lower radial stiffness than aluminum reference rings; however, the resulting deformations were elastic, repeatable and associated with stress levels below the material yield limit. External fixators equipped with printed rings demonstrated axial stiffness values within the range reported for conventional circular fixators used in clinical practice. In addition, the polymer-based configurations showed a notable reduction in mass and significantly improved radiographic transparency compared to metallic systems. *Conclusions*: Additively manufactured polymer rings with appropriately optimized geometry can provide mechanically acceptable performance for use in circular external fixators, while offering advantages in weight reduction and radiographic assessment.

Key words: *additive manufacturing, finite element method, biomechanical analysis, circular external fixator, polymer rings, mechanical stiffness*

1. Introduction

Circular external fixators, such as the classic Ilizarov apparatus, have long represented a cornerstone in the management of complex skeletal injuries and deformities. These devices are employed in procedures such as limb lengthening, multiplanar deformity correction, treatment of nonunions, stabilization of comminuted fractures and the management of severe open fractures, particularly those resulting from high-energy trauma often accompanied by substantial soft-tissue loss. A fundamental structural component of these systems is the ring, which whether in the form of complete or partial circular segments forms a three-dimensional fixation frame when connected with spacer or distraction rods. In combination with bone-anchored implants, the rings constitute a bone–fixator biomechanical construct that provides es-

* Corresponding author: Bartosz Martyniuk, Department of Mechanics, Materials and Biomedical Engineering, Wrocław University of Science and Technology, Wrocław, Poland. E-mail: Bartosz.martyniuk@pwr.edu.pl
Received: November 24th, 2025
Accepted for publication: January 28th, 2026

sential axial and radial stiffness, as well as resistance to bending and torsional loads [4], [5], [15].

Decades of advancement in ring external fixation technology have resulted in the development of successive device generations from the traditional Ilizarov apparatus (first generation), to hexapod-based systems (second generation), and more recently – to emerging multijointed configurations described as octopods (third generation). Although the overall architecture of these fixators has undergone considerable transformation, the design modifications applied specifically to the rings have been relatively modest. The existing literature identifies three principal directions in the evolution of ring components [4].

The first and arguably most consequential advancement was the transition from single to double-ring assemblies, a modification that substantially enhances construct stiffness under axial and shear loads, particularly when one of the bone segments being stabilized is short [6]. Subsequent improvements focused on the interfaces for securing implants and connecting struts: replacing the circumferential circular holes with longitudinal slots provided greater flexibility and precision in implant placement. However, reducing the amount of material in the ring inevitably diminished its structural integrity, potentially compromising its mechanical performance [13]. A third direction involved redesigning ring geometry by introducing additional external holes dedicated to the attachment of distraction rods. While this modification expanded the range of achievable fixation configurations, it also increased the overall spatial dimensions of the external fixator [7].

Conventional Ilizarov rings are typically manufactured from stainless steel, a material that offers excellent strength and wear resistance, but contributes substantially to the overall weight of the construct. Efforts to reduce fixator mass have led to the use of lightweight alternatives, including aluminum and titanium alloys as well as fiber-reinforced composites containing carbon or glass fibers, all of which provide sufficient stiffness while significantly lowering component weight [3].

The growing adoption of additive manufacturing (3D printing) has prompted the emergence of studies exploring the feasibility of incorporating printed components into biomechanical applications. Moreover, recent finite element and experimental analyses of additively manufactured PLA structures, including bone repair scaffolds, have demonstrated the mechanical reliability of 3D-printed polymeric constructs and highlighted their sensitivity to geometry and process parameters [14]. These findings establish a relevant biomechanical foundation for investigating the applicability and mechanical optimization of PLA rings in external fixation systems. In a recent literature review, O'Connor et al. [11] identified only nine publications on this topic, underscoring the limited maturity of research in this domain. Notably, just one of these studies included experimental mechanical testing. In that study, a clamp-type fixator utilizing 3D-printed structural elements satisfied ASTM F1541 standards and exhibited biomechanical performance comparable to commercially available devices [8].

Several studies have also explored the potential of 3D printing for producing patient-specific fixator components derived from medical imaging data. Qiao et al. [12] introduced a modification of the Ilizarov system that incorporated a photosensitive-resin cylinder positioned between ring segments. This additively manufactured element contained precisely engineered channels for the placement of Schanz screws, thereby enabling accurate fracture reduction and stable fixation. Alqahtani et al. [1] performed a topological optimization of a shell-type fixator, aiming to decrease overall mass by strategically removing material from its central region. Li et al. [9] proposed a novel external fixation concept featuring adjustable stiffness. The design consisted of a 3D-printed shell composed of Voronoi patterns, whose individual elements could be selectively detached according to finite element analysis results in order to adjust the rigidity of the construct.

To date, the sole study evaluating the mechanical performance of 3D-printed fixator rings is the work by Badea et al. [2], who conducted finite element analyses of a hybrid external fixator incorporating rings fabricated from carbon-fiber-reinforced PLA. While the findings highlighted the substantial potential of additively manufactured components, the simulations also revealed that geometric refinement of the rings is necessary, as the applied preload of approximately 1000 N in the Kirschner wires resulted in stress levels exceeding permissible limits.

The scarcity of research examining the mechanical performance of additively manufactured rings and, more broadly, the biomechanical behavior of external fixators incorporating these components highlights a substantial unmet need in the current literature.

The objective of this study was to design and additively manufacture rings from the thermoplastic polymer PLA demonstrating the mechanical performance necessary for incorporation into an external fixation system used for pediatric lower-limb lengthening. A further goal was to reduce X-ray attenuation by the fixator components, thereby improving visualization of the regenerate within the distraction gap and enhancing the accuracy of radiographic assessment throughout the bone-lengthening process.

2. Materials and methods

Two structural variants of rings produced using fused filament fabrication (FFF) additive manufacturing with PLA filament (F3DFilament, Katowice, Poland) were evaluated. The ring designs were fabricated using a desktop 3D printer (Bambu X1E, Shenzhen, China). The variants differed in their cross-sectional geometry, featuring either an H-beam (H-type) or an I-beam (I-type) profile (Fig. 1). A commercially manufactured aluminum ring (alloy 7020), supplied by MASTERMED (Kraków, Poland), served as the reference specimen. This ring had an inner diameter of 150 mm, an outer diameter of 194 mm, and a thickness of 7 mm (Fig. 1a), and incorporated 44 uniformly distributed holes with a diameter of 7 mm. The additively manufactured PLA rings were designed with the same inner diameter (150 mm) and an outer diameter of 200 mm. Two height configurations were investigated: a low-profile design (20 mm for the H-type and 28 mm for the I-type) and a high-profile design with a height of 40 mm. Each PLA ring included 11 holes with a diameter of 7 mm. The high-profile variants were intended to replicate the functional behavior of the conventional double-ring configuration, which is frequently employed in clinical practice to enhance stabilization of longer bone segments [6].

The study was conducted in two stages. The first stage involved numerical finite element analyses (ANSYS Workbench) aimed at evaluating deformation patterns and stress distributions in the tested ring designs under applied loading conditions. In the second stage, experimental testing was performed on physical models of three external fixators assembled using conventional metallic rings as well as additively manufactured PLA rings of H-type and I-type design.

Functional analysis of the rings

Numerical simulations were performed to evaluate the structural integrity of the proposed ring designs. In clinical applications, bone fragments in limb lengthening procedures are connected to the external fixator frame using two primary types of implants: Kirschner wires and Schanz screws. Accordingly, two distinct loading configurations were considered. The first configuration represented radial loading corresponding to the pretension force F_R generated by a Kirschner wire. Boundary conditions were defined by restraining three degrees of freedom at nodes located within a localized region of the ring. A radially oriented load, directed toward the ring axis, was applied to nodes situated on the outer

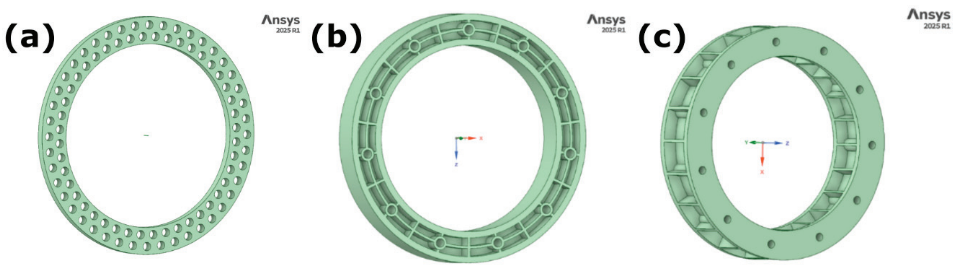

Fig. 1. Three-dimensional models of the investigated rings: (a) reference ring, (b) H-type ring, and (c) I-type ring

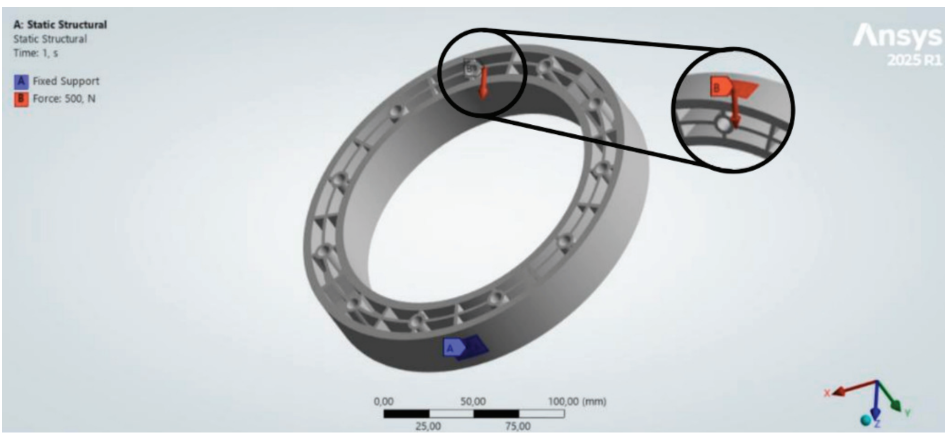

Fig. 2. Schematic representation of the applied load and boundary conditions used in the radial stiffness simulation, shown for the H-type ring

surface of the ring on the opposite side (Fig. 2). Given the intended use of the designed rings in paediatric external fixation systems, the applied force magnitude was assumed to be $F_R = 500$ N.

The second loading scenario considered an axial force applied along the ring axis to the free end of the Schanz screw. The implant was attached to the ring by means of a dedicated connector (Fig. 3). In this configuration, the primary region of interest was the vicinity of the ring–Schanz screw interface, where the highest levels of deformation and stress were anticipated. To reduce model complexity and computational cost, a half-ring model was employed. Boundary conditions were applied at the nodes located on the two cut surfaces resulting from sectioning the ring. One surface was fully constrained, with all translational degrees of freedom suppressed, whereas the opposite surface was constrained in the x and y directions, while displacement in the radial (z) direction was permitted. An axial load was applied to the nodes located at the free end of the Schanz screw. The applied force magnitude was set to 200 N, corresponding to the mean force generated by the tensile response of soft tissues surrounding the lengthened bone, as reported in the literature [5], [15]. To ensure a realistic representation of mechanical interactions, appropriate contact definitions were implemented. A nonlinear, frictionless contact ($\mu = \infty$) allowing separation was assigned between the connector and the ring hole, whereas a linear bonded contact was defined between the Schanz screw and the connector (Fig. 3). The material properties adopted for all components included in the numerical models are listed in Table 1.

Determination of external fixator stiffness

In the second stage of the study, external fixators were assembled using the additively manufactured rings in a configuration representative of clinical applications for the treatment of tibial length discrepancies. The reference fixator, incorporating conventionally manufactured aluminum alloy rings, consisted of a single proximal ring and a distal assembly composed of two rings. The distal rings were interconnected using short rods, providing an inter-ring spacing of 40 mm, while the proximal ring was connected to the distal assembly by four distraction rods. Two additional fixator configurations were constructed analogously using PLA rings fabricated by additive manufacturing. In the fixator employing H-type rings, a proximal ring with a height of 20 mm and a distal ring with a height of 40 mm were used. For the fixator incorporating I-type rings,

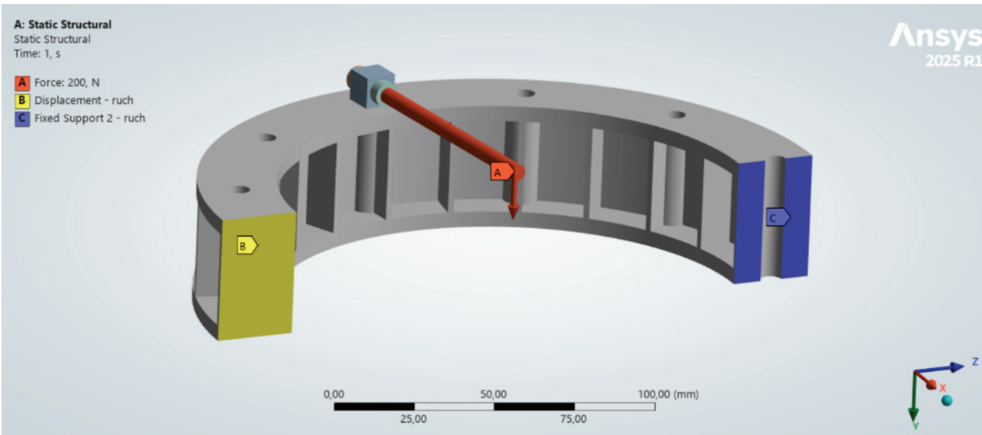

Fig. 3. Schematic representation of the applied load and boundary conditions used in the axial stiffness simulation for the I-type ring

Table 1. Mechanical properties of materials used in the numerical models

Component	Material	Young's modulus [GPa]	Poisson's ratio [–]	Yield strength [MPa]	Density [kg/m³]
Aluminum ring	Al 7020 alloy	70	0.33	140	2780
Additively manufactured rings	PLA	2.8	0.33	56.8	1292
Schanz screw	Ti–6Al–7Nb	110	0.37	800	4507
Schanz screw fixation components	AISI 304L stainless steel	193	0.33	190	7900

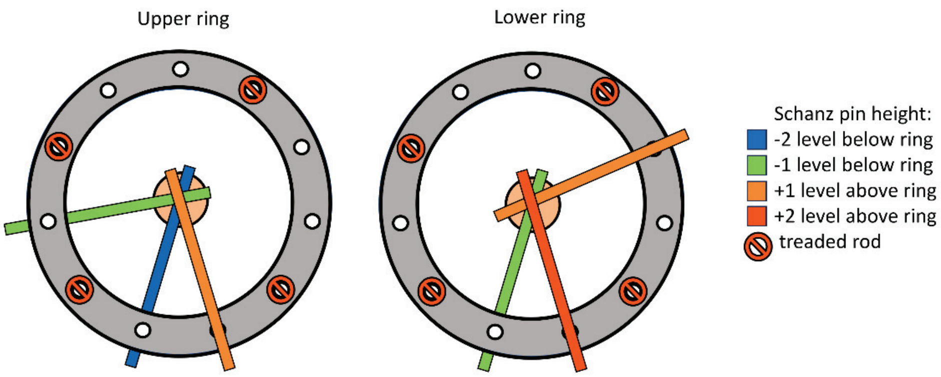

Fig. 4. Schematic illustration of the Schanz screw fixation between the rings and the tubular element

ring heights of 28 mm (proximal) and 40 mm (distal) were applied. In all configurations, four fully threaded M6 distraction rods were used, identical to those in the reference construct. Across all three fixator variants, Schanz screws with a diameter of 5 mm served as the bone–frame connecting implants. Three screws were inserted at each fixation level in the spatial arrangement illustrated in Fig. 4. The overall height of all tested fixators was maintained constant at 230 mm. The assembled fixators were mounted on a polypropylene (PP) tubular element, with an outer diameter of 32.5 mm, an inner diameter of 21 mm, and a length of 400 mm. To simulate the fracture or distraction gap, the tube was sectioned at its midpoint, creating a 10 mm gap.

Physical models of the external fixator–bone fragment assembly were mounted in a universal testing system (MTS 858 Mini Bionix, Minnesota, USA), which allowed for force measurement with a resolution of 0.1 N and displacement measurement with a resolution of 0.01 mm. The specimens were fixed using two spherical joints, enabling free rotation about three orthogonal axes (Fig. 5). The constructs were subjected to quasi-static axial loading. In the first loading step, an axial load was applied to induce a relative displacement of 0.5 mm between the bone fragments. Subsequently, the displacement was increased by an additional 4.5 mm. Upon reaching the prescribed displacement level, the loading direction was reversed, and the relative displacement was reduced back to 0.5 mm. This loading protocol was repeated for a total of 20 cycles.

Radiographic imaging assessment

To assess the influence of additively manufactured PLA rings on radiographic image quality, X-ray images of the physical models of the external fixator–bone fragment assemblies were acquired. Radiographic imaging was performed using a GMM EIDOS RF 439 system (Seriate, Italy) with the following acquisition parameters: tube voltage of 73 kV, dose–area product (DAP) in the range of 0.22–0.25 mGy·cm^2, and a current-time product of 0.8 mAs.

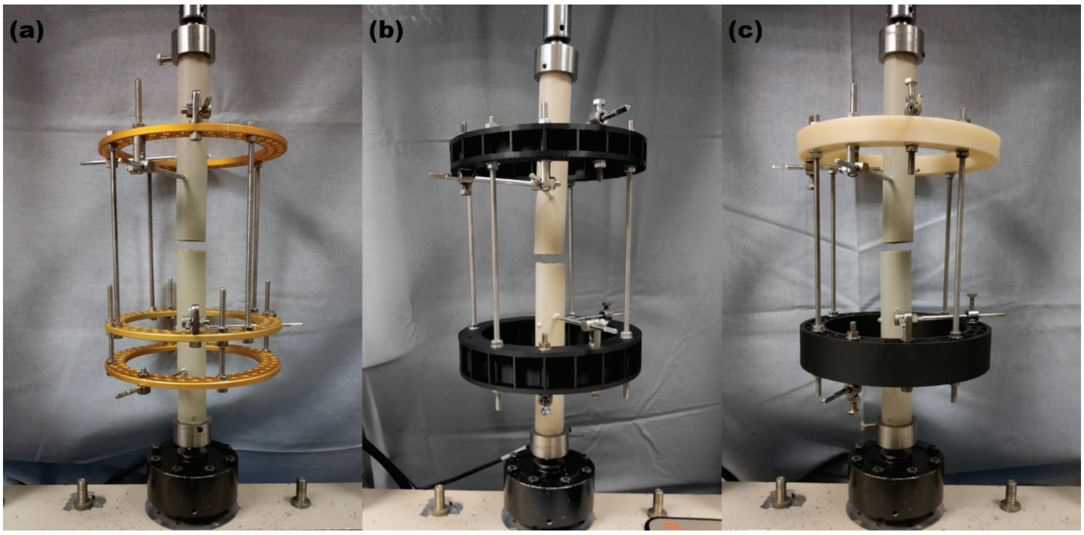

Fig. 5. External fixator–bone constructs mounted in the universal testing machine:
(a) reference configuration with aluminum rings, (b) fixator with I-type rings, and (c) fixator with H-type rings

3. Results

Finite element analyses of the tested rings under a radial load of F_R = 500 N were performed to evaluate the resulting deformation fields (Fig. 6) and the distribution of von Mises equivalent stress (Fig. 7).

Based on these results, the radial stiffness k_R was determined and defined as the ratio of the applied radial force F_R to the corresponding deformation of the ring measured in the load direction (Table 2).

The results demonstrate that the radial stiffness of the aluminum alloy ring was approximately one order of magnitude (5–10 times) higher than that of the PLA rings. Among the additively manufactured designs, the H-type rings exhibited superior radial stiffness compared with the I-type configuration. Although relatively large radial deformations were observed ranging from 1.06 to 1.34 mm for the H-type rings and from 1.72 to 1.94 mm for the I-type rings the deformation response remained fully elastic. This behaviour was confirmed by experimental tests in which the rings were subjected to repeated radial loading and unloading cycles in the force range of 200–900 N (Fig. 8). The force–displacement curves revealed a clear overlap between the loading and unloading paths over five successive cycles, indicating the absence of permanent deformation. Furthermore, the maximum von Mises equivalent stresses induced under these loading conditions remained below the yield strength of PLA (Table 2).

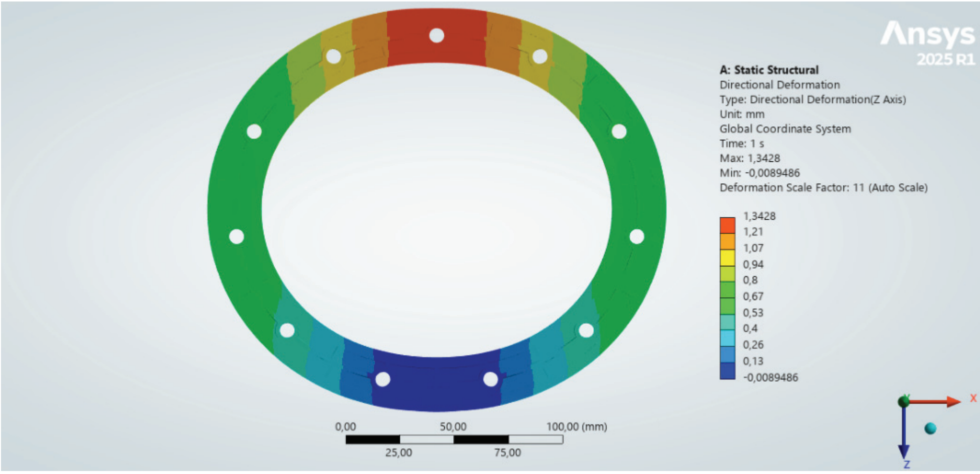

Fig. 6. An example of the displacement field in the *Z* direction for the H-type low ring under radial load

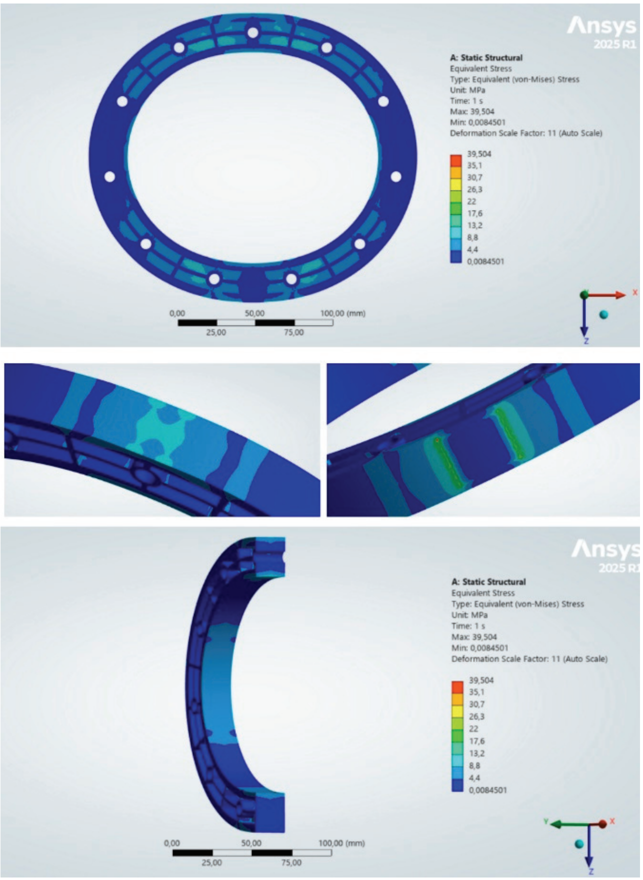

Fig. 7. Distribution of von Mises equivalent stress illustrated for the H-type low ring under radial load

Table 2. Radial stiffness of the rings determined by finite element analysis and the maximum von Mises equivalent stress values

Model	Radial stiffness (FEA) [N/mm]	maximum von Mises equivalent stress values (FEA) [MPa]
Reference ring	2520.2	57.27
I-type high	251.6	55.57
I-type low	291.3	25.42
H-type high	469.5	27.78
H-type low	372.4	39.50

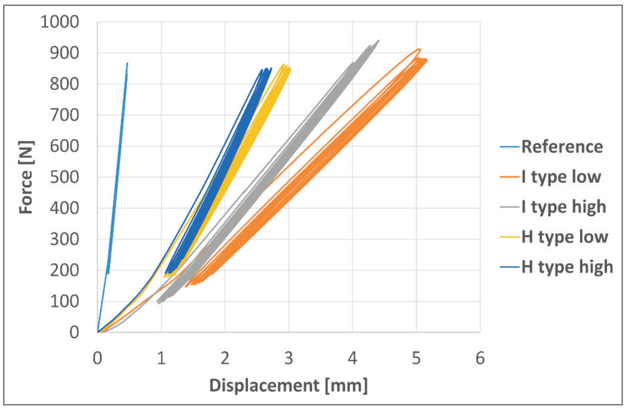

Fig. 8. Force–radial displacement relationship of the rings under cyclic loading conditions

In simulations involving axial loading applied through the Schanz screw, the highest equivalent stresses were observed at the screw–connector interface and within the fastening screw securing the connector to the ring. The interaction of these components with the ring generated equivalent stresses in the immediate contact region that remained below the yield strength of PLA. The maximum von Mises equivalent stress reached approximately 45 MPa for the H-type rings, whereas for the I-type rings the stress levels were substantially lower, not exceeding 20 MPa (Fig. 9).

The overall deflection of the rings was additionally evaluated and measured on their inner surfaces (Fig. 10). Maximum deflection was observed at the implant–ring interface. For each ring type, the magnitude of deflection was dependent on the ring height. Specifically, for the H-type rings, the taller variant exhibited a deflection of 0.31 mm, whereas the shorter variant reached 0.84 mm. In contrast, the I-type rings displayed lower deflections, all remaining below 0.5 mm.

Axial compression tests of the complete fixator assemblies were conducted to evaluate the relationship between the axial force F_A and the corresponding displacement of the bone fragments (Fig. 11). From these measurements, the axial stiffness k_A of the compared fixators was calculated. The reference fixator exhibited the highest axial stiffness at 48.06 N/mm. Fixators incorporating H-type and I-type polymer rings demonstrated comparable axial stiffness values of 37.17 and 35.25 N/mm, respectively (Table 3).

Table 3. Axial stiffness of external fixators assemblies: reference, I-type, H-type

External fixator configuration	Axial stiffness [N/mm]
Reference with aluminum rings	48.06
I-type rings	35.25
H-type rings	31.17

In comparative radiographic assessments, the proposed Ilizarov fixator designs featuring thermoplastic 3D-printed rings demonstrated superior radiolucency relative to the reference fixator with aluminum rings. Both configurations employing printed rings, especially I-type rings configuration showed enhanced radiographic trans-

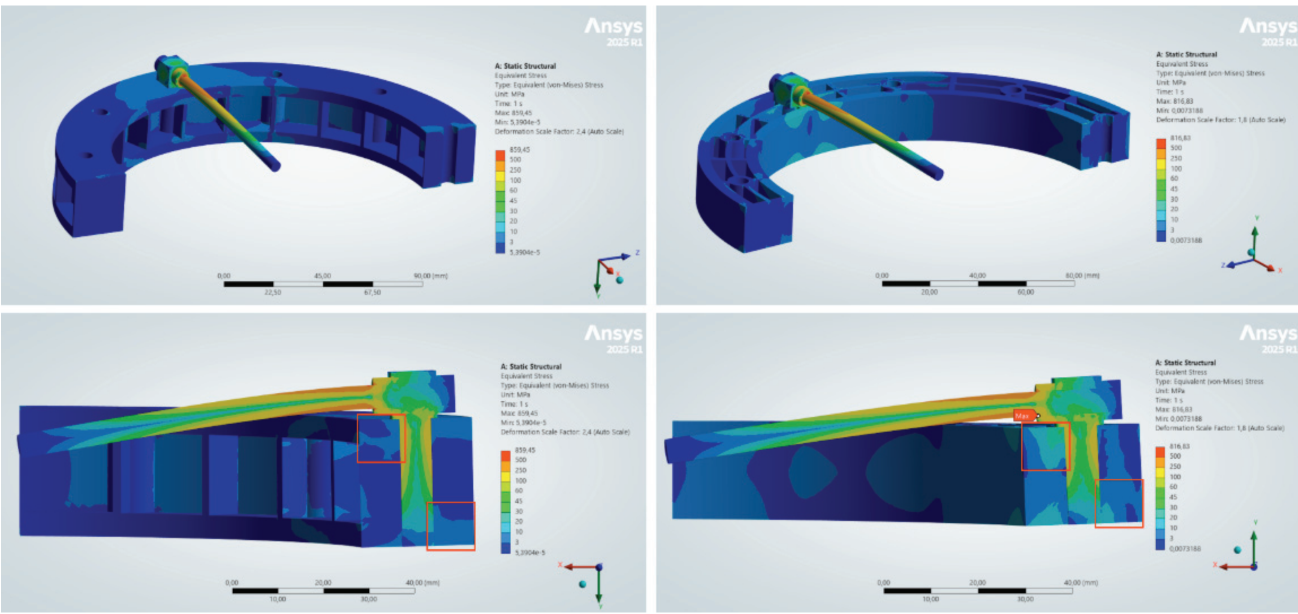

Fig. 9. Equivalent (von-Mises) stress of I-type low ring and H-type low ring under axial load. The regions of maximum stress in the rings are highlighted with a red square in the figure

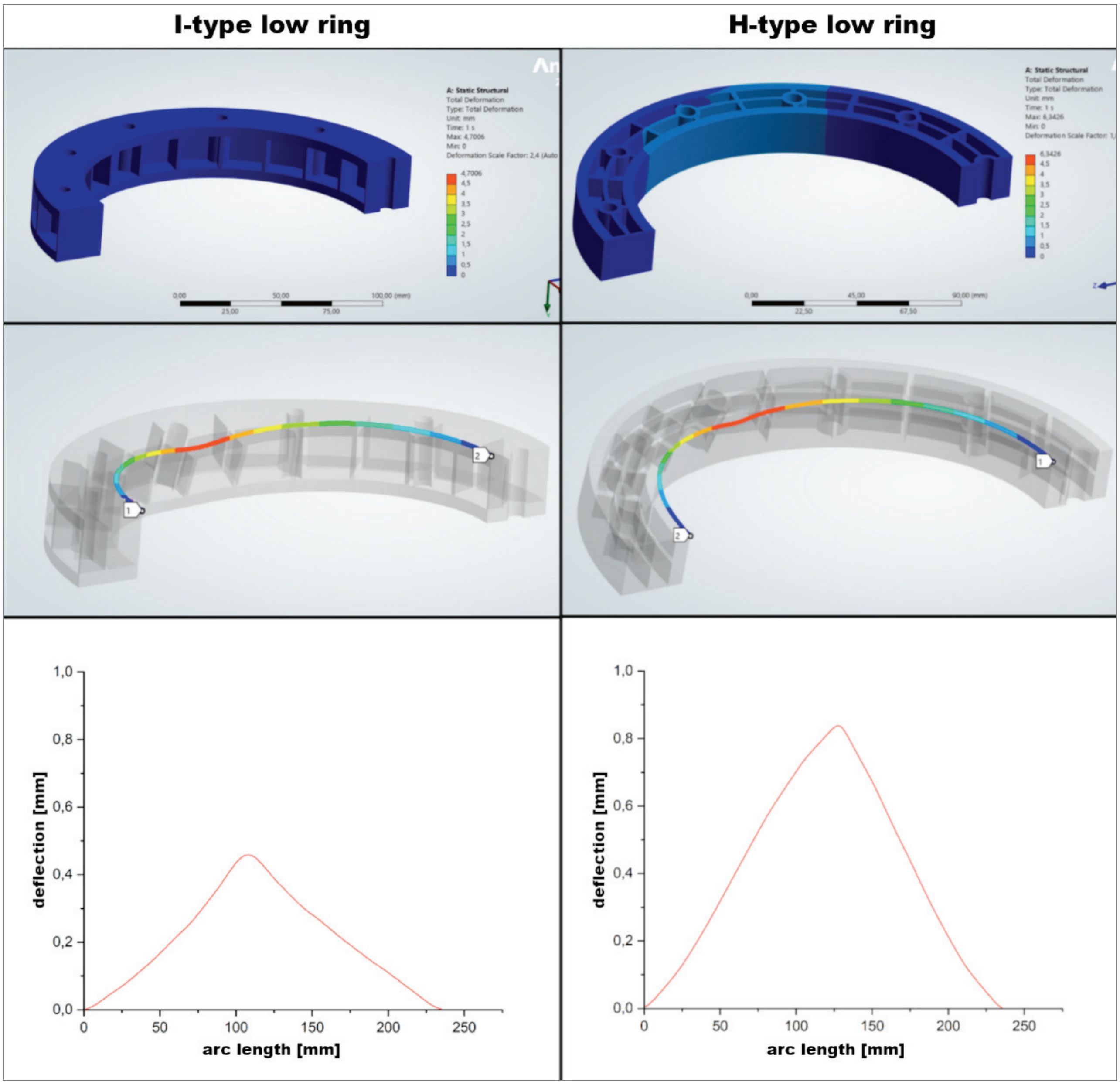

Fig. 10. Total deflection measured along the inner edge of the I-type low ring and the H-type low ring

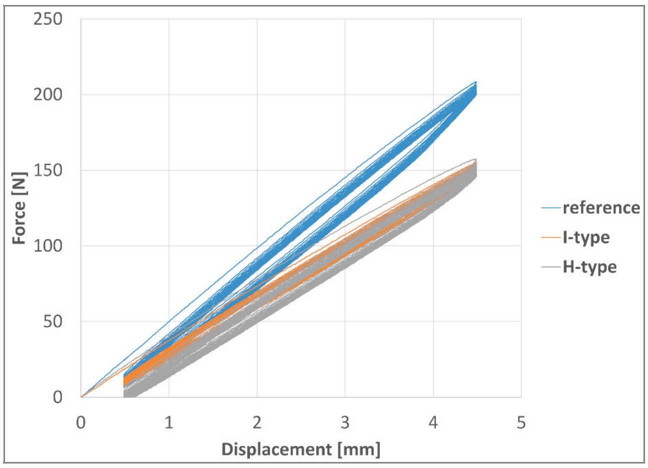

Fig. 11. Force–axial displacement relationship of the external fixator assemblies over 20 loading cycles

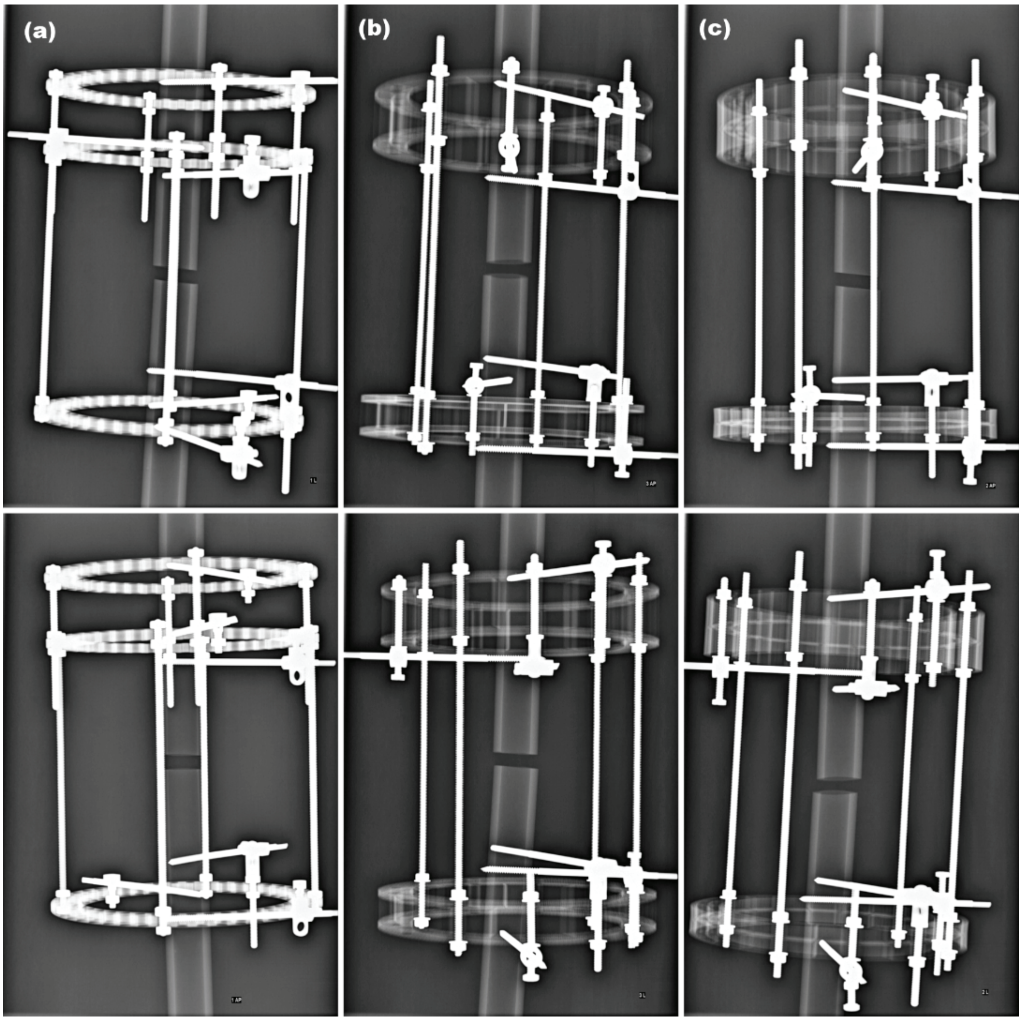

Fig. 12. Radiographic images of the fixators in anteroposterior (AP, top) and mediolateral (ML, bottom) orientations: (a) aluminum rings, (b) I-type rings, (c) H-type rings

parency and fewer visible structural components of the fixator on X-ray images compared to the conventional aluminum-ring configuration (Fig. 12).

4. Discussion

The present study aimed to evaluate the feasibility of employing FFF 3D-printed PLA rings in the fabrication of external fixators for the management of lower limb bone shortening and deformities in pediatric patients. Finite element simulations and experimental testing were used to characterize the mechanical properties of the FFF-manufactured rings and to assess the axial stiffness of fixators assembled from these rings.

The obtained results indicate that the radial stiffness of the aluminum ring is 5–10 times greater than that of the PLA rings. Despite relatively substantial radial deformations 1.06–1.34 mm for H-type rings and 1.72–1.94 mm for I-type rings the rings exhibited elastic behavior and maintained repeatability over successive loading cycles. Notably, the equivalent stresses observed in these loaded rings remained below the yield strength of PLA.

The axial stiffness of fixators incorporating FFF 3D-printed rings ranged from 35.25 to 37.17 N/mm, depending on the ring type, representing a 23–27% reduction relative to the reference fixator. These values are comparable to those reported in our previous investigations of conventional Ilizarov fixators, where axial stiffness varied between 29.53 and 35.96 N/mm depending on the implant configuration [10]. Similarly, Badea et al. [2] assessed PLA–carbon fiber composite rings as alternatives to metal rings, observing a 21–25% decrease in axial stiffness in their hybrid fixator while maintaining stresses within allowable limits under defined test scenarios. This suggests that polymer-based FFF-manufactured rings, when appropriately designed, can provide effective axial load transfer and satisfactory stabilization of bone fragments.

It is important to note that literature reports display substantial variability, reflecting differences in the tested fixators, material properties, and experimental protocols. O'Connor et al. [11] discuss this issue, emphasizing that such diversity limits direct comparisons and generalizations, and warrants caution when translating specific laboratory results into clinical practice. Nonetheless, these studies suggest that it is feasible to achieve biomechanical performance in fixators constructed from thermoplastic rings produced via additive manufacturing. Further refinement of manufacturing parameters and optimization of both the ring and overall fixator geometry are, however, required to maximize performance.

In addition to providing acceptable mechanical performance of rings produced via additive manufacturing and enabling their use in the construction of spatial fixators with programmable mechanical properties, other functional advantages were observed. The use of a low-density material such as PLA results in reduced X-ray attenuation compared to rings made of aluminum or austenitic steel. During limb lengthening or axis correction procedures, qualitative assessment of bone regenerate through radiographic imaging is crucial, particularly in the context of limb shortening treatment. Ilizarov fixators, especially in cases of multi-planar or multi-level deformity corrections, often exhibit complex three-dimensional architectures. The intricate spatial configuration and the large number of metallic components including rings, connectors, threaded rods, Kirschner wires, and Schanz pins can partially or substantially hinder radiographic evaluation and the monitoring of lengthening and axis correction processes. This issue is particularly relevant when applying Ilizarov fixators to relatively small limbs, such as in pediatric patients or individuals with short stature, where radiographic assessment of bone regenerate and deformity correction may be further complicated. For orthopedic surgeons performing treatment with the Ilizarov method, accurate evaluation of radiographs during the course of therapy is essential to assess the quality of bone regenerate formation and monitor progress in limb lengthening and deformity correction. It is well established that X-ray attenuation depends on both the material's chemical composition and its density. Metals exhibit high X-ray attenuation, whereas polymers, with densities approximately four times lower than aluminum alloys and composed of low atomic number elements such as carbon, hydrogen, and oxygen, display significantly lower attenuation. Moreover, the attenuation of PLA is lower than that of bone tissue. The rings produced in this study may therefore offer advantages over standard aluminum or steel components in Ilizarov treatment. Additively manufactured rings can provide diagnostic benefits by facilitating clearer and more comprehensive radiographic evaluation. Clinically, these rings may improve the precision of limb lengthening and deformity correction monitoring, as well as enable more accurate assessment of bone regenerate formation. Collectively, these advantages have the potential to enhance treatment outcomes and reduce the risk of complications associated with Ilizarov therapy.

Another significant advantage is the reduction in the mass of the fixator components achieved by replacing the dual-ring module made of aluminum with a high H-type or I-type ring. The mass of these rings, 264 g and 302 g, respectively, is lower than that of the two locked aluminum rings comprising the conventional dual-ring module (396 g). Importantly, the functional capability of the dual-ring module is preserved, allowing the spatial configuration of the implants to be adjusted according to the specific clinical requirements of individual patients. The reduction in external fixator mass is particularly relevant in the context of pediatric applications.

5. Conclusions

The results of the study confirm the potential for the effective use of plastic rings produced via FFF additive manufacturing for the construction of external fixators. Rings with the proposed H-type and I-type cross-sectional geometries exhibit mechanical properties that provide a favorable stress distribution under the loads typically encountered during the treatment of limb shortening, particularly in pediatric patients. The stresses observed do not exceed the material's allowable yield stress. External fixators constructed with such rings demonstrate axial stiffness comparable to that of conventional circular fixators. Additionally, they offer a realistic opportunity to reduce the overall mass of the fixator, which is especially important in pediatric applications.

Due to the low X-ray attenuation of polymers, imaging parameters can be optimized to achieve more effective visualization of the developing bone regenerate and to assess its biological quality. Although this aspect was not specifically addressed in the present study, the potential functionality that has not previously been exploited in external fixators, namely, the ability to design rings tailored to the individual needs of specific patients is worth noting. Additive manufacturing enables rapid and efficient production of such customized rings. Our observations align with trends reported in the literature, indicating that additive manufacturing technologies offer promising benefits, including reduced costs and personalization potential, while requiring careful material and geometric optimization and thorough mechanical validation prior to clinical application.

Further studies are warranted to evaluate the applicability of 3D-printed rings in Ilizarov treatment, including the assessment of a wider variety of printed ring designs and the determination of their durability under prolonged, cyclically varying loads. Definitive verification of the potential benefits related to enhanced radiographic imaging of the elongation site and newly forming bone tissue requires testing on cadaveric limb models.

References

[1] ALQAHTANI M.S., AL-TAMIMI A.A., HASSAN M.H., LIU F., BARTOLO P., *Optimization of a patient-specific external fixation device for lower limb injuries*, Polymers (Basel), 2021, 13 (16), 2661, DOI: 10.3390/polym13162661.

[2] BADEA I., ALEXANDRU T.G., POPESCU D., *Feasibility and mechanical performance of three dimensional printed polymer composite external fixators for tibial fractures*, Appl. Sci., 2025, 15, 4007, DOI: 10.3390/app15074007.

[3] COSSARD C., KUCIEL S., MAZURKIEWICZ S., LIBER-KNEĆ A., *Possibility of using polyamide 6 reinforced with glass fiber for Ilizarov rings*, Polimery, 2022, 53 (4), 317–320.

[4] DICKWELLA WIDANAGE K.N., DE SILVA M.J., LALITHARATNE T., BULL A.M., GOPURA R.A.R.C., *Developments in circular external fixators: a review*, Injury, 2023, 54, 111157, DOI: 10.1016/j.injury.2023.111157.

[5] FILIPIAK J., KRAWCZYK A., MORASIEWICZ L., *Distribution of radiological density in bone regenerate in relation to cyclic displacements of bone fragments*, Acta Bioeng. Biomech., 2009, 11 (3), 3–9.

[6] GRIVAS T.B., MAGNISSALIS E.A., *The use of twin-ring Ilizarov external fixator constructs: application and biomechanical proof-of-principle with possible clinical indications*, J. Orthop. Surg. Res., 2011, 6, 41, DOI: 10.1186/1749-799X-6-41.

[7] HERBERT C., SIVARASU S., *Design and development of an adaptive bone fracture fixation system*, Proc. ASME Des. Med. Devices Conf., 2019, V001T06A007, DOI: 10.1115/DMD2019-3276.

[8] LANDAETA F.J., SHIOZAWA J.N., ERDMAN A., PIAZZA C., *Low cost three dimensional printed clamps for external fixators for developing countries: a biomechanical study*, 3D Print Med., 2020, 6, 31, DOI: 10.1186/s41205-020-00082-3.

[9] LI H., LI D., QIAO F., TANG L., HAN Q., *Three dimensional printing adjustable stiffness external fixator for mechanically stimulated healing of tibial fractures*, Biomed. Res. Int., 2021, 2021, 8539416, DOI: 10.1155/2021/8539416.

[10] MARTYNIUK B., MORASIEWICZ P., WUDARCZYK S., DRAGAN S.F., FILIPIAK J., *The impact of configuration of the Ilizarov fixator on its stiffness and the degree of loading of distraction rods*, Clin. Biomech., 2019, 63, 79–84, DOI: 10.1016/j.clinbiomech.2019.02.020.

[11] O'CONNOR H.A., ADAMS L.W., MACFADDEN L.N., SKELLEY N.W., *Three dimensional printed orthopaedic external fixation devices: a systematic review*, 3D Print Med., 2023, 9, 15, DOI: 10.1186/s41205-023-00164-0.

[12] QIAO F., LI D., JIN Z., GAO Y., ZHOU T., HE J., *Application of three dimensional printed customized external fixator in fracture reduction*, Injury, 2015, 46 (6), 1150–1155, DOI: 10.1016/j.injury.2015.03.017.

[13] TOMANEC F., RUSNÁKOVÁ S., KALOVÁ M., MANAS L., *Innovation of Ilizarov stabilization device with design changes*, MM Sci. J., 2019, 3, 2732–2738.

[14] VÁSQUEZ D., MEDINA L., MARTÍNEZ G., *Mechanical analysis and sensitivity evaluation of polylactic acid scaffolds for bone tissue repair using finite element analysis and Taguchi experimental design*, Acta Bioeng. Biomech., 2025, 27 (1), 69–81, DOI: 10.37190/ABB-02572-2024-03.

[15] VIJAYAKUMAR V., MARKS L., BREMNER-SMITH A., HARDY J., GARDNER T., *Load transmission through a healing tibial fracture*, Clin. Biomech., 2006, 21 (1), 49–53, DOI: 10.1016/j.clinbiomech.2005.08.010.